Nanoparticle-Mediated Expression of an Angiogenic Inhibitor Ameliorates Ischemia-Induced Retinal Neovascularization and Diabetes-Induced Retinal Vascular Leakage

Kyoungmin Park,[1] Ying Chen,[1] Yang Hu,[1] Aaron S. Mayo,[2] Uday B. Kompella,[2] Richard Longeras,[1] and Jian-xing Ma[1]

OBJECTIVE—The aim of the study is to evaluate the effect of nanoparticle-mediated gene delivery of angiogenic inhibitors on retinal inflammation, vascular leakage, and neovascularization in diabetic retinopathy.

RESEARCH DESIGN AND METHODS—An expression plasmid of plasminogen kringle 5 (K5), a natural angiogenic inhibitor, was encapsulated with poly(lactide-coglycolide) to form K5 nanoparticles (K5-NP). Expression of K5 was determined by Western blot analysis and immunohistochemistry, and retinal vascular leakage was measured by permeability assay. Retinal neovascularization was evaluated using fluorescein-angiography and counting preretinal vascular cells in rats with oxygen-induced retinopathy. Effects of K5-NP on retinal inflammation were evaluated in streptozotocin-induced diabetic rats by leukostasis assay and Western blot analysis of intracellular adhesion molecule and vascular endothelial growth factor. Possible toxicities of K5-NP were evaluated using histology examination, retinal thickness measurement, and electroretinogram recording.

RESULTS—K5-NP mediated efficient expression of K5 and specifically inhibited growth of endothelial cells. An intravitreal injection of K5-NP resulted in high-level expression of K5 in the inner retina of rats during the 4 weeks they were analyzed. Injection of K5-NP significantly reduced retinal vascular leakage and attenuated retinal neovascularization, when compared with the contralateral eyes injected with Control-NP in oxygen-induced retinopathy rats. K5-NP attenuated vascular endothelial growth factor and intracellular adhesion molecule-1 overexpression and reduced leukostasis and vascular leakage for at least 4 weeks after a single injection in the retina of streptozotocin-induced diabetic rats. No toxicities of K5-NP were detected to retinal structure and function.

CONCLUSIONS—K5-NP mediates efficient and sustained K5 expression in the retina and has therapeutic potential for diabetic retinopathy. ***Diabetes*** **58:1902–1913, 2009**

From the [1]Department of Medicine, Department of Cell Biology, University of Oklahoma Health Sciences Center, Oklahoma City, Oklahoma; and the [2]Department of Pharmaceutical Sciences, University of Nebraska Medical Center, Omaha, Nebraska.

Corresponding author: Jian-xing Ma, jian-xing-ma@ouhsc.edu.

Received 27 September 2008 and accepted 4 May 2009.

Published ahead of print at http://diabetes.diabetesjournals.org on 2 June 2009. DOI: 10.2337/db08-1327.

K.P. and Y.C. contributed equally to this study.

Retinal vascular leakage and neovascularization are the major features of diabetic retinopathy and the leading causes of vision loss (1–3). These retinal vascular abnormalities are also common in other ocular disorders such as sickle cell retinopathy, retinal vein occlusion, and retinopathy of prematurity (1,4,5). Vascular endothelial growth factor (VEGF) plays a key pathogenic role in the blood-retinal barrier breakdown or vascular leakage and retinal neovascularization (6–8).

Angiogenesis is regulated by two counter-balancing systems between angiogenic stimulators, such as VEGFs and angiogenic inhibitors such as angiostatin (4,9,10). Angiostatin contains the first four triple disulfide bond-linked loops of plasminogen known as kringle domains and is a potent inhibitor of angiogenesis (11). Among proteolytic fragments of plasminogen, kringle 5 (K5), an 80–amino acid peptide from plasminogen, has the most potent inhibitory effect on endothelial cell growth (12). Previously, we have shown that K5 inhibits ischemia-induced retinal neovascularization in the oxygen-induced retinopathy (OIR) model (13). K5 also reduces retinal vascular leakage in the OIR model and in the streptozotocin (STZ)-induced diabetes model (14). The K5-induced reduction of vascular leakage is achieved through an intraocular, periocular, topical, or systemic administration of the K5 peptide (15). Similar to that of many other anti-angiogenic peptides, however, these K5 effects are transient after a single injection of the K5 peptide because of its short half-life in the retina (14,15). A sustained ocular delivery of K5, such as gene therapy, is desirable for the development of a long-term treatment of diabetic retinopathy.

Traditionally, gene delivery systems can be classified into viral vector-mediated and nonviral deliveries. Currently, viral vectors are the most commonly used means for gene delivery because of their high efficiencies (16,17). The limitations of viral vector-mediated delivery, such as potential risks, restricted targeting of specific cell types, and immunogenecity of viral vectors hamper their clinical application (18,19). For these reasons, nonviral systems for gene delivery have become increasingly desirable in both basic research and clinical settings.

One of the emerging nonviral vector-mediated gene delivery systems is condensation of plasmid DNA or oligonucleotides into nanoparticles (20). There are several biocompatible polymers to be used for DNA delivery, such

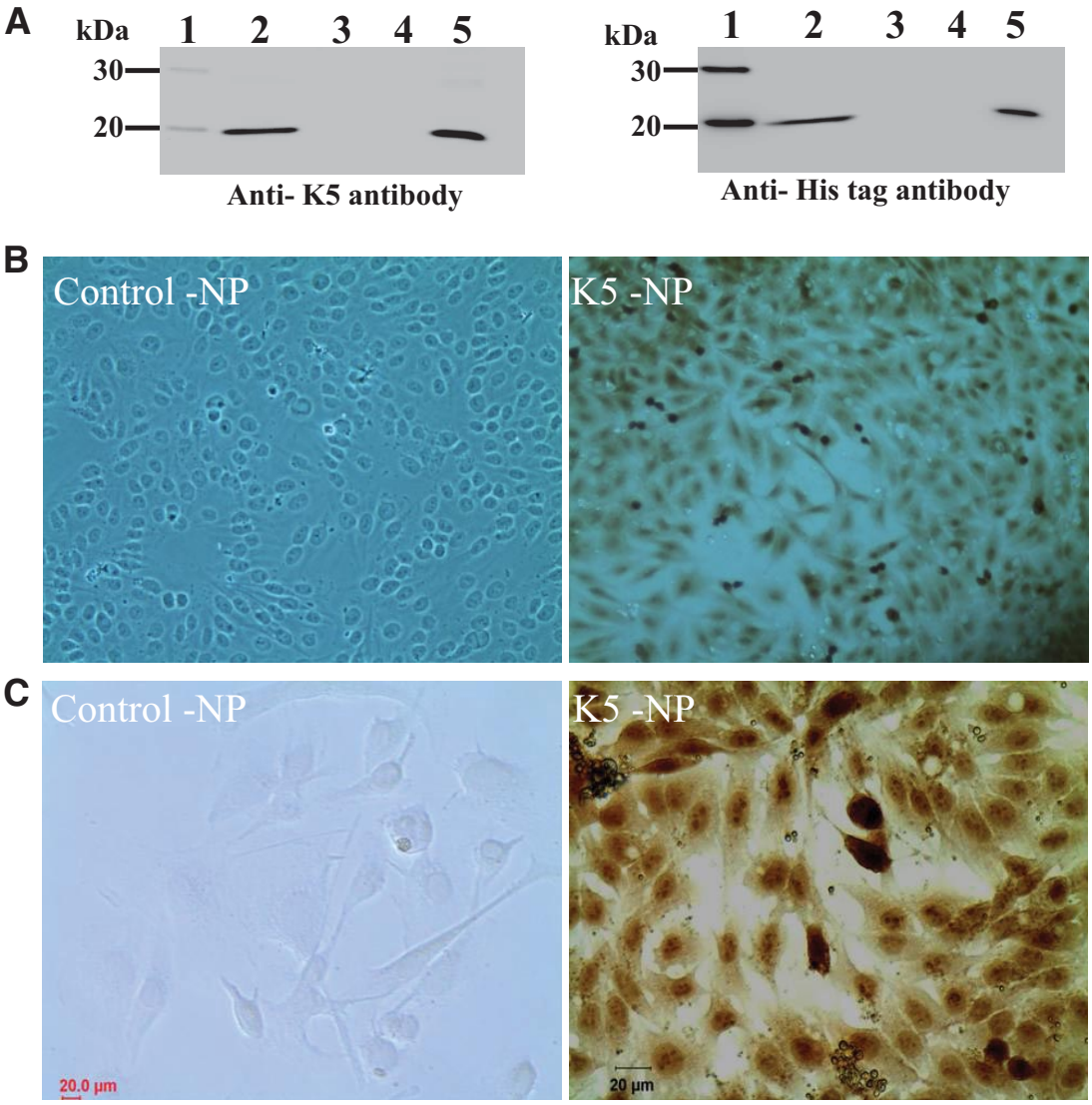

FIG. 1. K5 expression from K5-NP in vitro. ARPE19 cells were grown to 70% confluence in a medium containing 5% FBS. The culture medium was replaced by a serum-free medium. Control-NP and K5-NP were separately added into the medium to 1 μg/ml (plasmid DNA concentration) and incubated with the cells for 72 h. *A*: The medium was collected and concentrated. Total protein concentrations in the media were measured using the Bradford assay. The same amount of total proteins (20 μg) was applied for Western blot analysis separately using an antibody specific for human K5 and an anti–His-tag antibody. *Lane 1*, molecular weight markers; *lane 2*, medium from cells treated with K5-NP; *lane 3*, untreated cells; *lane 4*, treated with control-NP; *lane 5*, purified K5 peptide as positive control. *B* and *C*: ARPE19 cells were grown overnight on glass slides, treated with K5-NP and control-NP at 1 μg/ml for 72 h, washed, and fixed. The cells were immunostained with a monoclonal antibody against the His-tag using a 3,3′-diaminobenzidine color reaction that shows brown color in cells with positive immunostaining. *B*: 100×, *C*: 400×. (A high-quality digital representation of this figure is available in the online issue.)

as poly(D,L-lactide-coglycolide) (PLGA) and poly(ethylene-covinyl acetate) (EVAc). Several groups have successfully encapsulated naked DNA into biodegradable PLGA nanoparticles for long-term and controlled DNA release (21). Although matrix-type nanoparticles have been formulated using different polymers, the nanoparticles formulated from PLGA are especially of interest for gene delivery because of their safety, biocompatibility, biodegradability, and sustained release characteristics (22,23).

We encapsulated an expression plasmid of K5 with PLGA polymer to form nanoparticles and evaluated the efficacy of these K5 nanoparticles (K5-NP) on ischemia-induced retinal vascular leakage and retinal neovascularization in the OIR rat model. We evaluated the effects of K5-NP on retinal inflammation in STZ-induced diabetic rats. In addition, we also tested the ocular toxicities of K5-NP.

RESEARCH DESIGN AND METHODS

Construction of expression vector for K5. The human K5 cDNA (362 bp) was amplified by PCR using a pair of primers containing a 6× histidine tag (His-tag) at the COOH-terminus of K5. For secretion of K5, a 52-bp linker encoding the signal peptide was cloned into a pcDNA3.1(+). The amplified K5 cDNA with the His-tag sequence was subcloned into pcDNA3.1(+) vector at the *Bam*HI and *Xba*I sites in frame with the signal peptide sequence. The resulting pcDNA3.1(+)-SP-K5–6×His-tag expression construct was confirmed by restriction digestion and DNA sequencing.

Preparation and characterization of PLGA:Chitosan pK5-NPs

Preparation of PLGA:Chitosan pK5-NPs. PLGA:Chitosan nanoparticles containing the K5 expression plasmid (PLGA:CHN pK5-NPs) were prepared using a previously reported emulsion-diffusion evaporation technique (24) with some modifications. Briefly, 15.5 mg PLGA (50:50, 0.17 i.v.; Birmingham Polymers) was dissolved in 5 ml ethyl acetate. The polyvinyl acetate solution (1%, wt/vol) was prepared and then chitosan chloride (Nova Matrix PCL 113, 2.5 mg) was stirred until dissolved. Plasmid solution (1 ml containing 350 μg plasmid) was modified with 10% (wt/vol) sodium sulfate and added to the chitosan solution for complexation and DNA

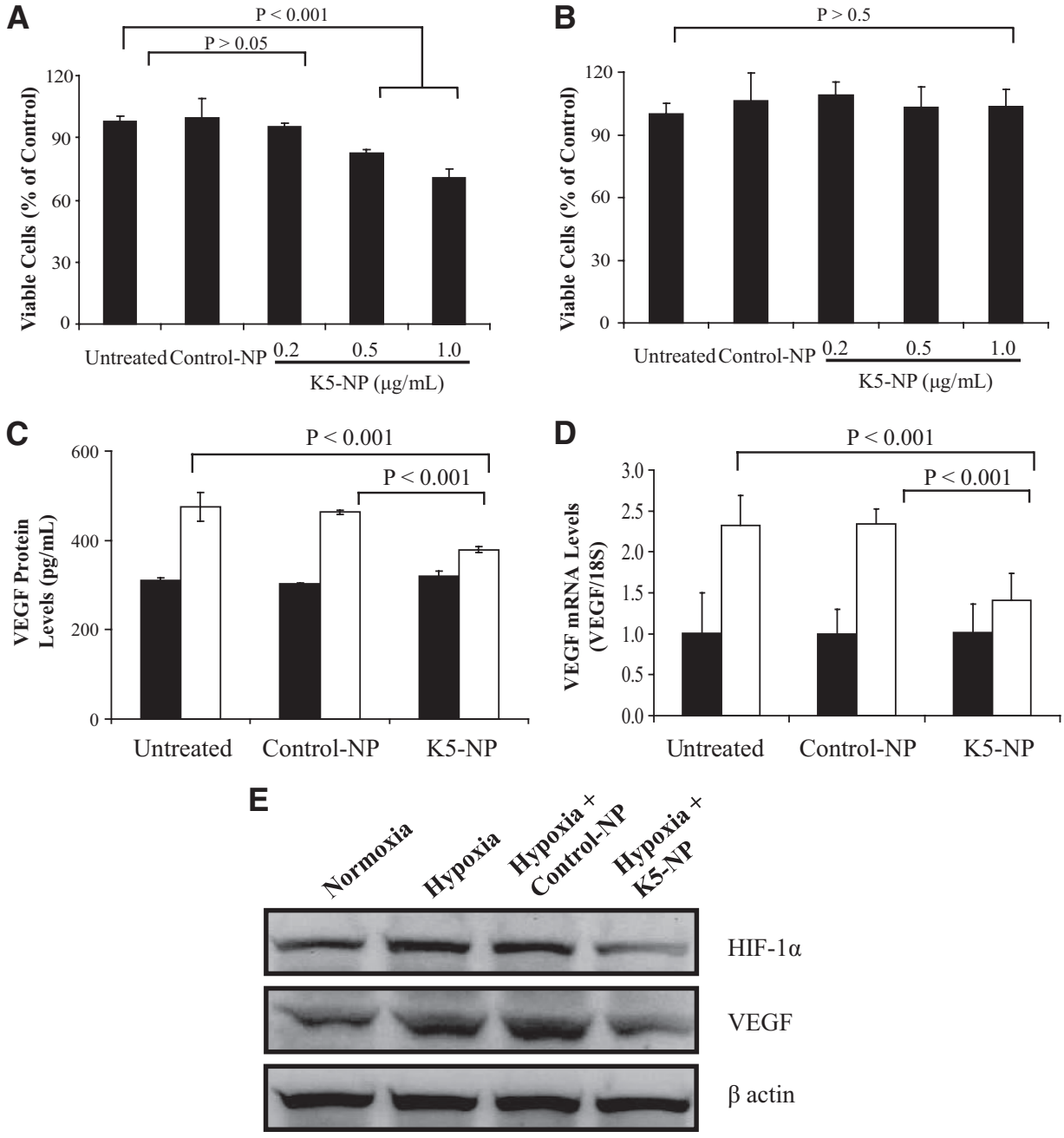

FIG. 2. Inhibitory effect of K5-NP on endothelial cell growth and VEGF overexpression under hypoxia. *A*: BRCECs grown in media containing 1% FBS were treated with K5-NP at the concentrations as indicated for 72 h. The viable cells were quantified using the MTT assay. K5-NP induced a dose-dependent decrease of cell viability in BRCECs. *B*: At the same concentrations, K5-NP did not inhibit ARPE19 cell growth. *C*: ARPE19 cells were treated separately with 1 μg/ml control-NP and K5-NP for 72 h. The culture medium was replaced with a serum-free medium, and the cells were exposed to hypoxia for 24 h. VEGF secreted into the medium was measured by ELISA using an ELISA kit (R&D Systems, Minneapolis, MN) and normalized by total protein concentrations in the medium. *D*: Total RNA was extracted from the treated ARPE19 cells, and VEGF mRNA levels were quantified by RT-PCR and normalized by 18S rRNA levels. Values are mean ± SD (n = 3). □, Hypoxia; ■, normoxia. *E*: Müller cells were treated separately with 1 μg/ml control-NP and K5-NP for 72 h. The culture medium was replaced with a serum-free medium, and the cells were exposed to hypoxia for 24 h. VEGF and HIF-1α levels were analyzed by immunoblotting and normalized by β-actin levels.

condensation and stirred. Both solutions were then combined and emulsified with a probe sonicator for 4 min. To the emulsion, ~30 ml Milli-Q H_2O was added and stirred on a magnetic plate stirrer for 3 h to evaporate the solvent. The particle suspension was ultracentrifuged and resuspended in Milli-Q H_2O, and the procedure was repeated twice. Upon final resuspension in Milli-Q H_2O, the nanoparticle suspension was lyophilized to obtain dry particles.

Particle size and ζ-potential measurement. The particle size and size distribution were determined using dynamic light scattering (Brookhaven Instruments, Holtsville, NY). The same equipment was used to determine the ζ-potential of the particles.

Estimation of plasmid loading in nanoparticles. For plasmid loading estimation, the lyophilized product (0.2 mg) was dispersed in 1 ml methylene chloride to dissolve the polymer, followed by extraction of the plasmid into 2 ml Tris-EDTA buffer. An aliquot of the Tris-EDTA buffer fraction was analyzed for the absorbance at 260 nm to determine the plasmid content per milligrams of nanoparticles.

Western blot analysis. For in vitro assay, protein extracts were prepared from a human Müller cell line (MIO-M1) (a generous gift from Drs. Khaw and Limb [25]) and treated with Control-NP or K5-NP under hypoxia for 48 h. For in vivo assay, the free-floating retinas were homogenized in 150 μl ice-cold tissue lysis buffer (50 mmol/l Tris-HCl, pH 7.4, 2 mmol/l $MgCl_2$, 1% NP-40, 10%

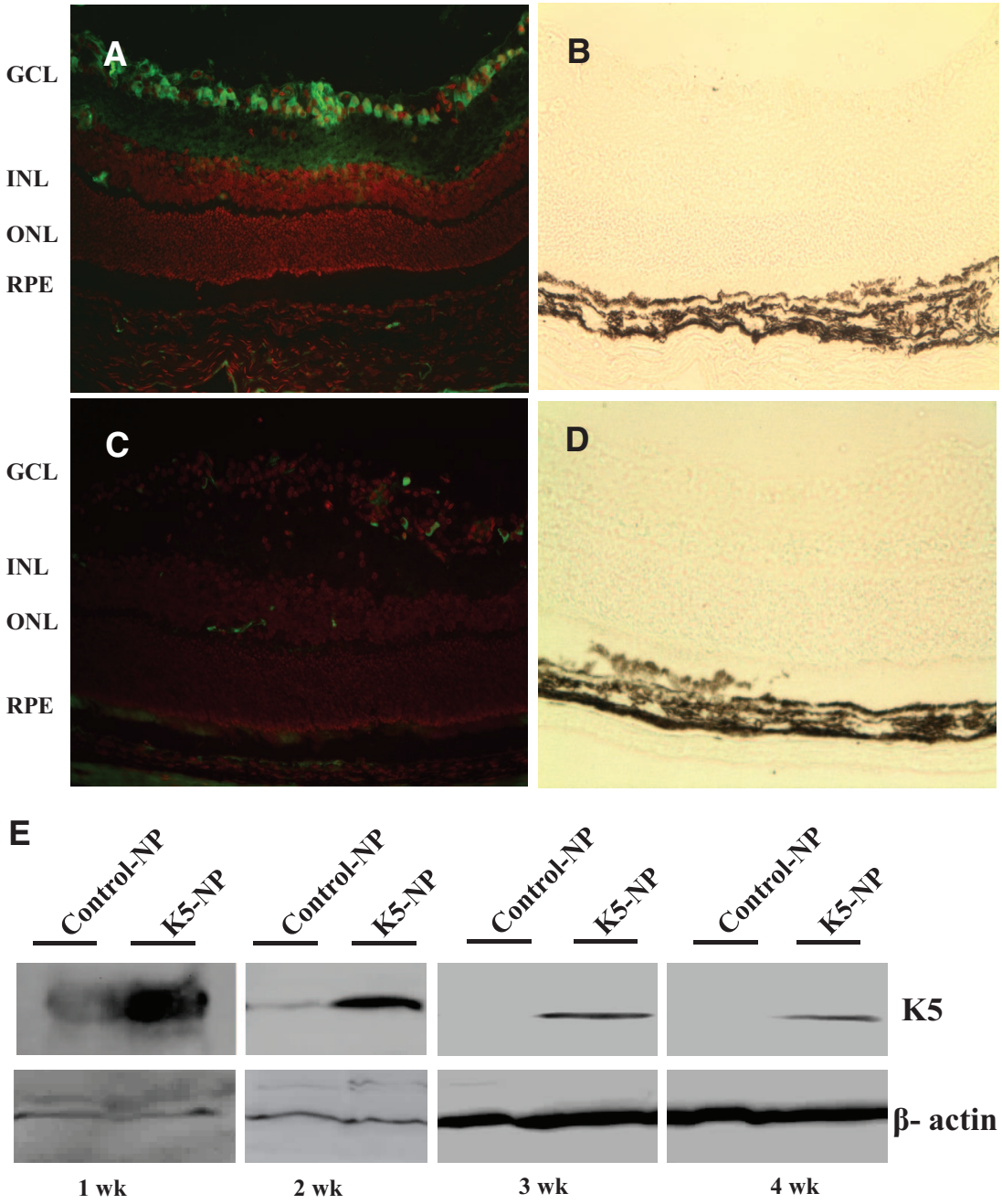

FIG. 3. K5 expression in the rat retina after an intravitreal injection of K5-NP. *A–D*: K5-NP was injected into the vitreous of the right eyes and control-NP into the contralateral eyes of four OIR rats at P12. K5 expression was examined at P18 by immunohistochemistry in ocular sections using an anti–His-tag antibody (green). The nuclei were counterstained with DAPI (red). *A* and *C*: Representative immunostaining images from the eyes injected with K5-NP (*A*) and control-NP (*C*). *B* and *D*: Phase contrast images of the same areas shown in *A* and *C*, respectively. Scale bar: 20 μm. *E*: K5-NP and control-NP were separately injected into the vitreous. The retinas were dissected at 1, 2, 3, and 4 weeks after the injection of K5-NP or control-NP (three rats per time point). The same amount of proteins (100 μg) from each retina was loaded for Western blot analysis using the anti–His-tag antibody. The same membrane was striped and re-blotted with an anti–β-actin antibody. No K5 expression was found in the retinas injected with control-NP, whereas K5 expression was detected in all of the retinas with the K5-NP injection. GCL, ganglion cell layer; INL, inner nuclear layer; ONL, outer nuclear layer; RPE, retinal pigment epithelium. (A high-quality digital representation of this figure is available in the online issue.)

glycerol, 100 mmol/l NaCl) and a protease inhibitor cocktail (1:100 dilution, Sigma Aldrich, St. Louis, MO) added just before use. The lysates were cleared by centrifugation at 12,000 *g* for 20 min at 4°C. The protein concentration of the lysate was determined using the Bradford assay. The same amount of proteins (50 μg) were resolved by SDS-PAGE in 8% denaturing gels and transferred onto nitrocellulose membranes. Ponceau S staining (Sigma Aldrich) was carried out to verify equal protein loading. Immunoblotting and signal detection by enhanced chemiluminescences were performed as described previously by incubating the membranes with the primary antibodies against rabbit anti-VEGF (1:1,000 in 5% nonfat milk powder/0.1% TBS Tween-20, Santa Cruz), HIF-1α (1:1,000; BD Transduction Laboratories), goat anti-ICAM-1 (1:1,000; Santa Cruz), mouse anti–His-tag (1:2,000; Upstate), mouse anti-TATA box-binding protein (TATA-binding protein [TBP], 1:1,000; Abcam), or mouse anti–β-actin (1:2,000; Abcam) antibodies overnight at 4°C. The signal intensity was quantified by densitometry using software (SynGene, Frederick, MD).

Immunohistochemistry. Immunostaining was performed as described previously (26). Briefly, the eyes were cross-sectioned vertically through the center of the cornea and optic nerve, and both halves of the eyeball were embedded with the center facing down. Serial cryosection (5 μm thickness) was blocked with 10% goat serum in 0.1% Triton X-100 and 3% BSA in PBS. After PBS washes, the antibody specific for the His-tag was added and

incubated with the sections at 4°C overnight. The sections were rinsed several times with PBS and incubated with a fluorescein isothiocyanate conjugated anti-mouse IgG antibody for 1 h. The slides were then rinsed in cold PBS and viewed under a fluorescence microscope.

Real-time RT-PCR. The reverse transcription and real-time PCRs (RT-PCR) were performed as described previously (26). The primers used for human VEGF (5′ CAGAGCGGAGAAAGCATTTG and 3′ TGGTTCCCGAAACCCTG AGG) amplified a 180-bp fragment of VEGF. The 18S rRNA was amplified using primers (5′ TGCTGCAGTTAAAAAGCTCGT and 3′ GGCCTGCTTTG AACA CTCTAA) for normalization of the VEGF mRNA levels.

Rat models of OIR and STZ-induced diabetes. All the animal experiments were performed in compliance with the ARVO Statement for the Use of Animals in Ophthalmic and Vision Research. Brown Norway rats (Charles River Laboratories) were used for the OIR model following an established protocol (27). OIR rats received an intravitreal injection of K5-NP into the right eye and the same dose of Control-NP into the left eye at age of P12. Diabetes was induced and monitored in adult Brown Norway rats by an intraperitoneal injection of STZ (50 mg/kg in 10 mmol/l of citrate buffer, pH 4.5) as described previously (14,28). Diabetic rats at 2 weeks after the onset of diabetes received an intravitreal injection of Control-NP and K5-NP in the treatment group and the same dose of Control-NP in the control group.

Retinal vascular permeability assay. Retinal vascular permeability was measured using the Evens blue-albumin leakage assay following an established protocol (29). Concentrations of Evans blue in the retina were normalized by total retinal protein concentrations and by Evans blue concentrations in the plasma.

Fluorescein retinal angiography and quantifying preretinal vascular cells. Retinal vasculature was visualized by fluorescein angiography as described (13,27). The neovascular area was measured in the retina using SPOT software (Diagnostic Instruments, Sterling Heights, MI). For quantification of preretinal vascular cells, eyes were fixed, sectioned, and stained as described previously (27). The preretinal nuclei were counted, averaged, and compared using Student's *t* test.

Electroretinogram recording. Rats were dark adapted for at least 12 h. The rats were killed and pupils dilated with topical application of 2.5% phenylephrine and 1% tropicamide. Electroretinogram (ERG) responses were recorded with a silver chloride needle electrode placed on the surface of the cornea after 1% tetracaine topical anesthesia. A reference electrode was positioned at the nasal fornix and a ground electrode on the foot. The duration of light stimulation was 10 ms. The band pass was set at 0.3–500 Hz. Fourteen responses were recorded and averaged with flash intervals of 20 s. For quantitative analysis, the B-wave amplitude was measured between A- and B-wave peaks. The ERG waveforms of both eyes in the same animal were simultaneously recorded and compared using the right-to-left eye ratio of B-wave amplitude.

Measurement of nuclear levels of hypoxia-inducible factor-1. Nuclear and cytosolic fractions were isolated using the Fractionation System Kit (Biovision, Mountain View, CA). Nuclear and cytosolic protein concentrations were measured using the Bradford assay. The proteins were blotted with an antibody specific for hypoxia-inducible factor-1 (HIF-1α; Santa Cruz Biotechnology, Santa Cruz, CA) at 1:500 dilution.

RESULTS

Characteristics of K5-NP. Nanoparticle size, polydispersity index, ζ-potential, and plasmid loading were measured with four different nanoparticle batches, and various parameters are shown below (mean ± SD). The nanoparticle formulation exhibited a mean hydrodynamic diameter of 260 ± 30 nm, a polydispersity index of 0.28 ± 0.005, ζ-potential of 8.4 ± 2.4 mV, and a plasmid loading of 11 ± 1.4 μg/mg particles.

K5 expression from K5-NP in cultured cells. ARPE19 cells were transfected with 10 μg of K5-NP or Control-NP for 3 days. The concentrated conditioned serum-free medium from the transfected cells was blotted separately with the anti-K5 and anti–His-tag antibodies. Both of the antibodies detected significant amounts of K5 with the expected molecular weight secreted from the cells transfected with K5-NP, but not from the cells transfected with Control-NP (Fig. 1*A*).

The K5 expression was also determined by immunocytochemistry using the anti–His-tag antibody. The antibody detected K5 signal in the cells transfected with K5-NP, but not in the cells transfected with Control-NP (Fig. 1*B* and *C*).

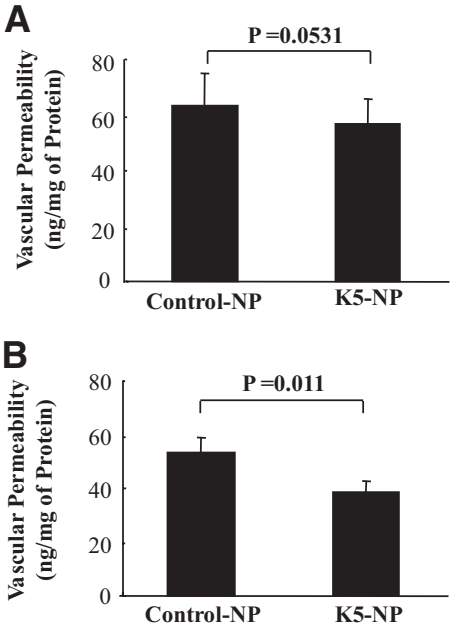

FIG. 4. Effect of K5-NP on retinal vascular leakage in OIR rats. OIR rats received an intravitreal injection of 2.2 μg (*A*) or 8.8 μg (*B*) of K5-NP into the right eyes and the same dose of control-NP into the left eyes at P12. Retinal vascular permeability was measured using the Evans blue-albumin leakage method at P16. The vascular leakage was normalized by total protein concentrations in the retina, averaged within the group (mean ± SD, $n = 7$) and compared with contralateral eyes using paired Student's *t* test. The eyes injected with 8.8 μg of K5-NP showed a significantly lower retinal vascular permeability compared with the contralateral eye ($P = 0.011$) (*B*).

Specific inhibition of endothelial cell growth and VEGF overexpression by K5-NP. To determine the biological effect of K5-NP, primary bovine retinal capillary endothelial cells (BRCECs) and ARPE19 cells were treated with K5-NP for 3 days, and viable cells were quantified using the MTT assay. As shown in Fig. 2*A* and *B*, K5-NP induced a dose-dependent decrease in viable BRCEC numbers, when compared with the untreated cells and the cells treated with Control-NP (Fig. 2*A*). In contrast, the same K5-NP treatment did not result in significant reduction of viable cells in ARPE19 (Fig. 2*B*), suggesting that the inhibitory effect of K5-NP on cell growth is endothelial cell–specific.

Our previous studies showed that K5 inhibits angiogenesis via downregulation of VEGF expression (30). Here we evaluated the effect of K5-NP on VEGF expression by measuring VEGF secretion and VEGF mRNA levels. As shown by ELISA, ARPE19 cells overexpressed VEGF after exposure to hypoxia (1% O_2). K5-NP treatment significantly reduced the VEGF secretion induced by hypoxia, to a level comparable to that from the cells under normoxia (Fig. 2*C*). Similarly, RT-PCR showed that K5-NP significantly downregulated the VEGF mRNA expression under hypoxia, whereas Control-NP did not affect VEGF expression under the same conditions (Fig. 2*D*).

The effects of K5-NP were also evaluated in cultured rMc-1, a cell line derived from rat retinal Müller cells (31). As shown by Western blot analysis, K5-NP attenuated the overexpression of VEGF and decreased HIF-1α levels in Müller cells cultured under hypoxia (1% O_2) (Fig. 2*E*).

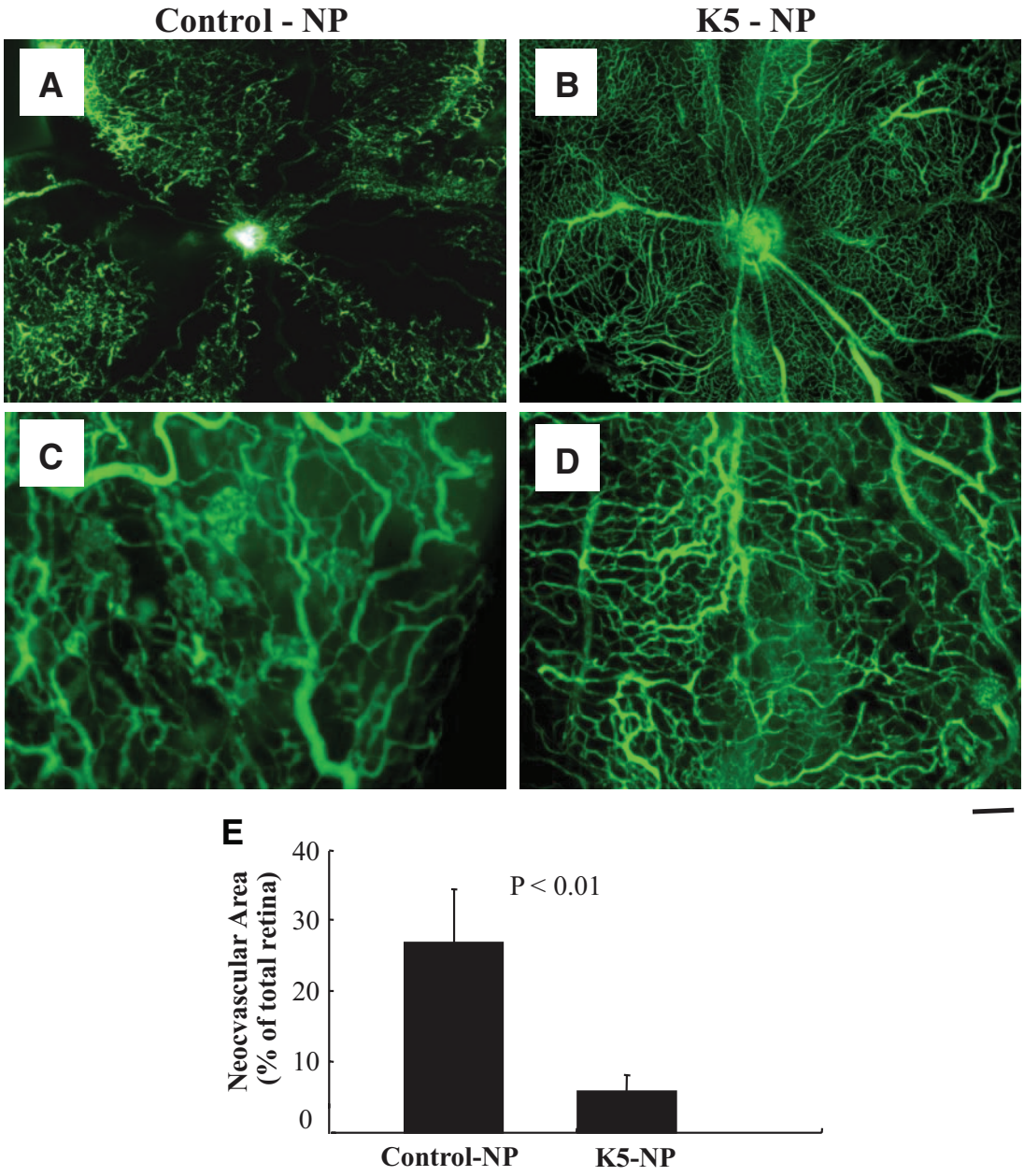

FIG. 5. Effect of K5-NP on retinal neovascularization in OIR rats. K5-NP was injected into the vitreous of the right eyes (8.8 μg/eye) and the same amount of control-NP into the contralateral eyes of seven OIR rats at P12. Retinal vasculature was examined using fluorescein angiography at P18 as described in METHODS. *A* and *C*: Representative retinal angiographs from the eyes injected with control-NP; *B* and *D* are representative angiographs from the K5-NP–injected eyes (40× in *A* and *B*; 100× in *C* and *D*). Scale bar: *A* and *B*, 100 μm; *C* and *D*, 40 μm. *E*: Retinal neovascularization was quantified by measuring the neovascular area in the retina and expressed as percent of the total retina area (mean ± SD, *n* = 7). The difference of the neovascular area was compared with the contralateral eyes using paired Student's *t* test. (A high-quality digital representation of this figure is available in the online issue.)

Sustained expression of K5 in the retina after an intravitreal injection of K5-NP. To examine the expression of K5 from K5-NP in the retina, K5-NP was injected into the vitreous of the right eye (8.8 μg/eye) and the same amount of Control-NP into the left vitreous of four OIR rats at age of postnatal day 12 (P12) after exposure to 75% oxygen. At age P18, the immunohistochemistry was performed on retinal sections using the anti–His-tag antibody. The immunostaining detected high levels of K5 expression in the inner retina in the eyes injected with K5-NP, but not in the contralateral control eyes (Fig. 3*A*–*D*).

To determine the duration of the K5 expression after a single injection of K5-NP, the retinas were dissected and homogenized at 1, 2, 3, and 4 weeks after an intravitreal injection of K5-NP in adult rats (three rats per time point) for Western blot analysis using the anti–His-tag antibody. K5 was detected with an expected molecular weight in the retinas injected with K5-NP at all the time points analyzed (Fig. 3*E*), but not in the retinas injected with the Control-NP.

K5-NP reduces retinal vascular leakage in OIR rats. To evaluate the effect of K5-NP on retinal vascular leakage, K5-NP was injected intravitreally into the right eye (2.2 or 8.8 μg/eye) at age P12 and the same amount of Control-NP into the contralateral eyes. Retinal vascular leakage was measured at P16 using the Evans blue-albumin leakage

method and compared with the contralateral eyes. The results showed that the eyes injected with 8.8 μg of K5-NP had significantly lower vascular permeability than that in the contralateral retinas injected with Control-NP ($P = 0.011$, $n = 7$; Fig. 4*B*). The injection of 2.2 μg of K5-NP did not result in a statistically significant decrease of vascular leakage ($P = 0.0531$, $n = 7$; Fig. 4*A*).

K5-NP inhibits ischemia-induced retinal neovascularization. To evaluate the effect of K5-NP on retinal neovascularization, K5-NP was injected intravitreally into the right eyes (8.8 μg/eye) of the OIR rats at P12 and Control-NP into the left eyes. The retinal vasculature was visualized and examined by fluorescein retinal angiography at P18. Retinal angiographs on retinal flat mounts showed that the eyes injected with Control-NP developed severe retinal neovascularization in the OIR rats (Fig. 5*A* and *C*). In contrast, a single K5-NP injection ameliorated the retinal neovascularization in the same rats by decreasing neovascular areas and nonperfusion areas in the retina (Fig. 5*B* and *D*). The neovascularization was semi-quantified by measuring the ratio of the neovascular area to the total retina area, which showed that the eyes injected with K5-NP have significantly decreased retinal neovascular areas in the OIR rats, compared with those injected with Control-NP (Fig. 5*E*).

The effect of K5-NP on preretinal neovascularization was also quantified by counting vascular cells growing into the vitreous space (preretinal vascular cells) on eight noncontinuous cross-sections from each eye following an established method (27). The result showed that the eyes injected with K5-NP have significantly fewer preretinal neovascular cells, compared with the contralateral eyes injected with Control-NP (Fig. 6).

K5-NP reduces retinal vascular leakage and blocks expression of VEGF and ICAM-1 in STZ-induced diabetic rats. To determine the effect of K5-NP on retinal inflammation, K5-NP was injected intravitreally into STZ-induced diabetic rats, with the same dose of Control-NP as vehicle control. As VEGF and ICAM-1 are both known to play important roles in the retinal inflammation and blood-retinal barrier breakdown in diabetes, we measured retinal levels of ICAM-1 and VEGF from nondiabetic rats, STZ-induced diabetic rats, and diabetic rats treated with Control-NP and K5-NP using Western blot analysis. Four weeks after the injection, the retinas from rats injected with K5-NP showed decreased retinal VEGF and ICAM-1 levels by more than 50%, compared with that in the retina injected with Control-NP and to that in untreated diabetic rats (Fig. 7*A*). Consistently, leukostasis assay showed that K5-NP also decreased adherent leukocytes in the retinal vasculature of diabetic rats (supplementary Fig. 1, available in an online appendix at http://diabetes.diabetesjournals.org/cgi/content/full/db08-1327/DC1). Retinal vascular permeability in the retinas of nondiabetic and STZ-induced diabetic rats, and diabetic rats treated with Control-NP and K5-NP, was measured using the Evans blue-albumin leakage method. As shown by retinal vascular permeability assay, K5-NP reduced retinal vascular leakage by 30% in STZ-induced diabetic rats, 4 weeks after the injection of K5-NP ($P < 0.001$, Fig. 7*B*), suggesting that the effect of K5-NP on retinal vascular leakage lasted for at least 4 weeks after a single injection. In contrast, Control-NP injection did not result in any significant difference in retinal levels of VEGF and ICAM-1 or retinal vascular leakage in the diabetic rats.

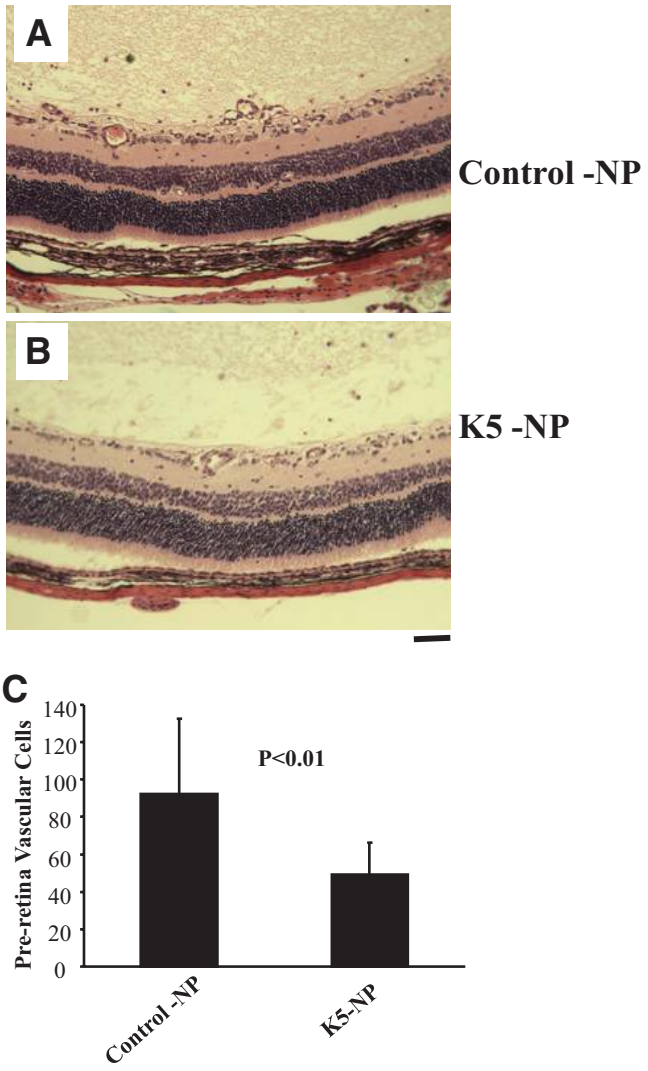

FIG. 6. Effect of K5-NP on preretinal neovascularization in OIR rats. K5-NP was injected intravitreally into the right eyes and control-NP into the left eyes of six OIR rats at P12. The eyes were fixed, sectioned, and stained with hematoxylin and eosin at P18. *A* and *B*: Representative sections from the eyes injected with control-NP (*A*) and from that with K5-NP (*B*) injection. Scale bar: 40 μm. *C*: Preretinal vascular cells were counted in eight noncontinuous sections per eye and averaged as described in RESEARCH DESIGN AND METHODS. The average numbers of preretinal vascular cells (mean ± SD, $n = 6$) were compared with the eyes injected with K5-NP and those with Control-NP using paired Student's *t* test. (A high-quality digital representation of this figure is available in the online issue.)

Lack of detectable toxicities to the structure and function of the retina. Possible toxicities of K5-NP were evaluated structurally by histological analysis. The eyes from rats with K5-NP injection and those with Control-NP injection were sectioned, stained, and examined under light microscope at 1, 2, and 4 weeks after the injection. No difference was observed in number of retinal nuclear layers or thickness of the retina among the rats injected with K5-NP and the control (Fig. 8*A*–*F*). We also measured the retinal thickness at the same six retinal locations in each eye as described in supplementary METHODS. There is no significant difference in retinal thickness in the rats treated with K5-NP and controls (supplementary Fig. 2, available in the online appendix). Similarly, K5-NP did not increase apoptotic cells in the retina (supplementary Fig. 3, available in the online appendix).

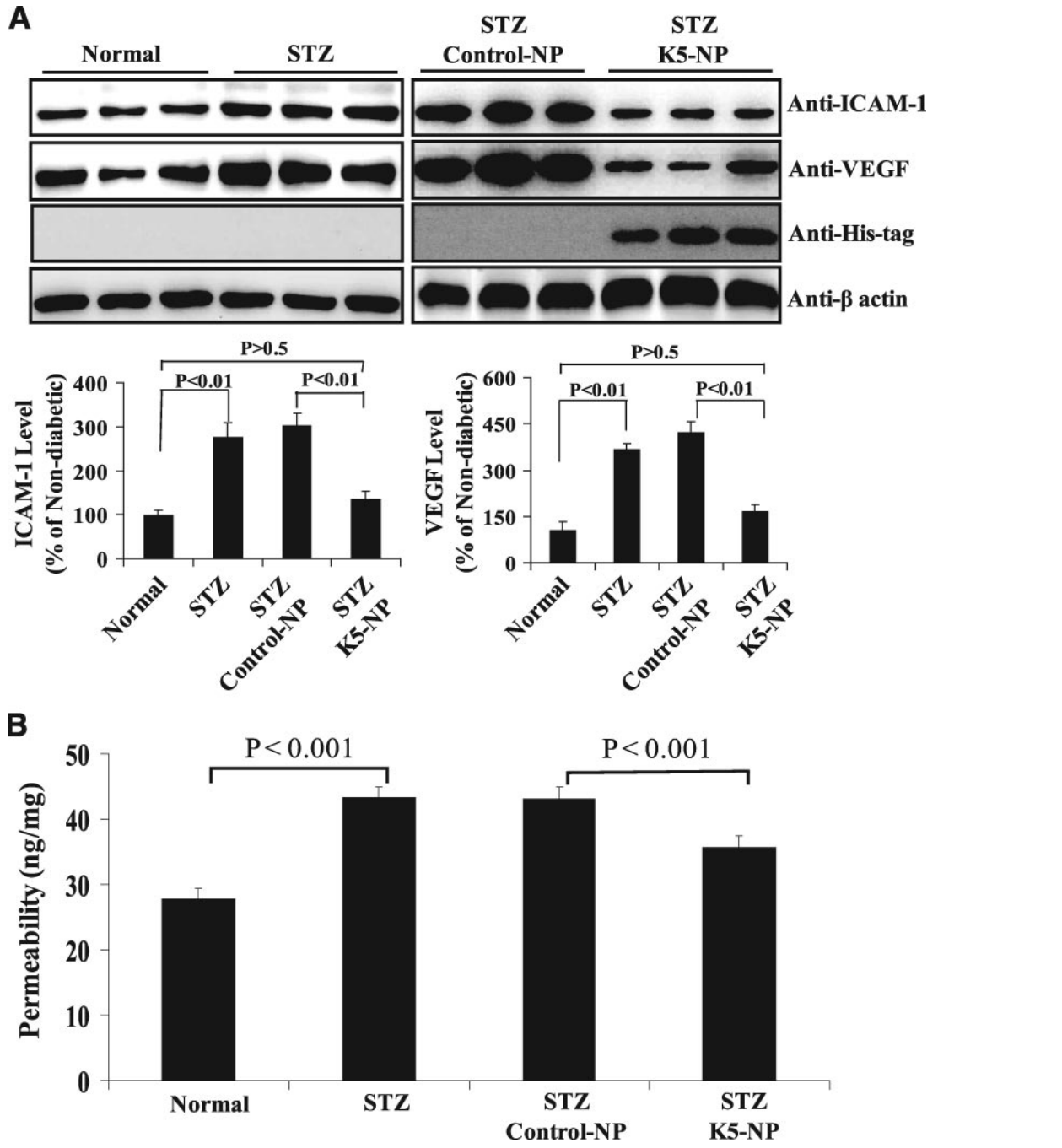

FIG. 7. Effect of K5-NP on retinal vascular leakage and expression of VEGF and ICAM-1 in diabetic rats. STZ-induced diabetic rats at 2 weeks after the onset of diabetes received an intravitreal injection of 5 μg/eye of K5-NP in the treatment group and the same dose of control-NP in the control group. *A*: Four weeks after the injection, retinal levels of ICAM-1 and VEGF from nondiabetic control, untreated diabetic rats, and diabetic rats treated with control-NP and K5-NP were determined using immunoblotting. The same membrane was stripped and re-blotted with the anti–His-tag and anti–β-actin antibodies. Retinal levels of VEGF and ICAM-1 in diabetic rats treated with control-NP and K5-NP were quantified by densitometry and expressed as percent of that in nondiabetic rat retinas (mean ± SD, $n = 3$). *B*: Retinal vascular permeability in the retina of nondiabetic rats, untreated diabetic rats, and diabetic rats treated with control-NP and K5-NP was measured using the Evans blue-albumin leakage method at 4 weeks after the injection of control-NP or K5-NP, normalized by the total protein concentration in the retina and the Evans blue concentration in the blood and expressed as nanogram dye per milligram of retinal proteins (mean ± SD, $n = 8$).

Possible adverse effects of K5-NP on visual functions were evaluated by ERG recording in normal and diabetic rats. As shown in Fig. 8, the amplitudes of A- or B-waves were not significantly different among the Control-NP or K5-NP treated rats and untreated rats. STZ-induced diabetic rats showed ERG responses similar to the nondiabetic rats (Fig. 8*G* and *H*).

K5-NP inhibits the activation of HIF-1. To investigate the mechanism responsible for the anti-angiogenic activity of K5-NP, we have measured the effect of K5-NP on HIF-1 activation, since HIF-1 is the key transcription factor activating VEGF and is known to play a key role in retinal neovascularization (7). HIF-1α nuclear translocation is a critical step in the activation of HIF-1, and thus, we measured cytosolic and nuclear levels of HIF-1α in the human Müller cell line treated with K5-NP under hypoxia. As shown by Western blot analysis of isolated nuclear proteins, exposure of the cells to hypoxia (1% oxygen)

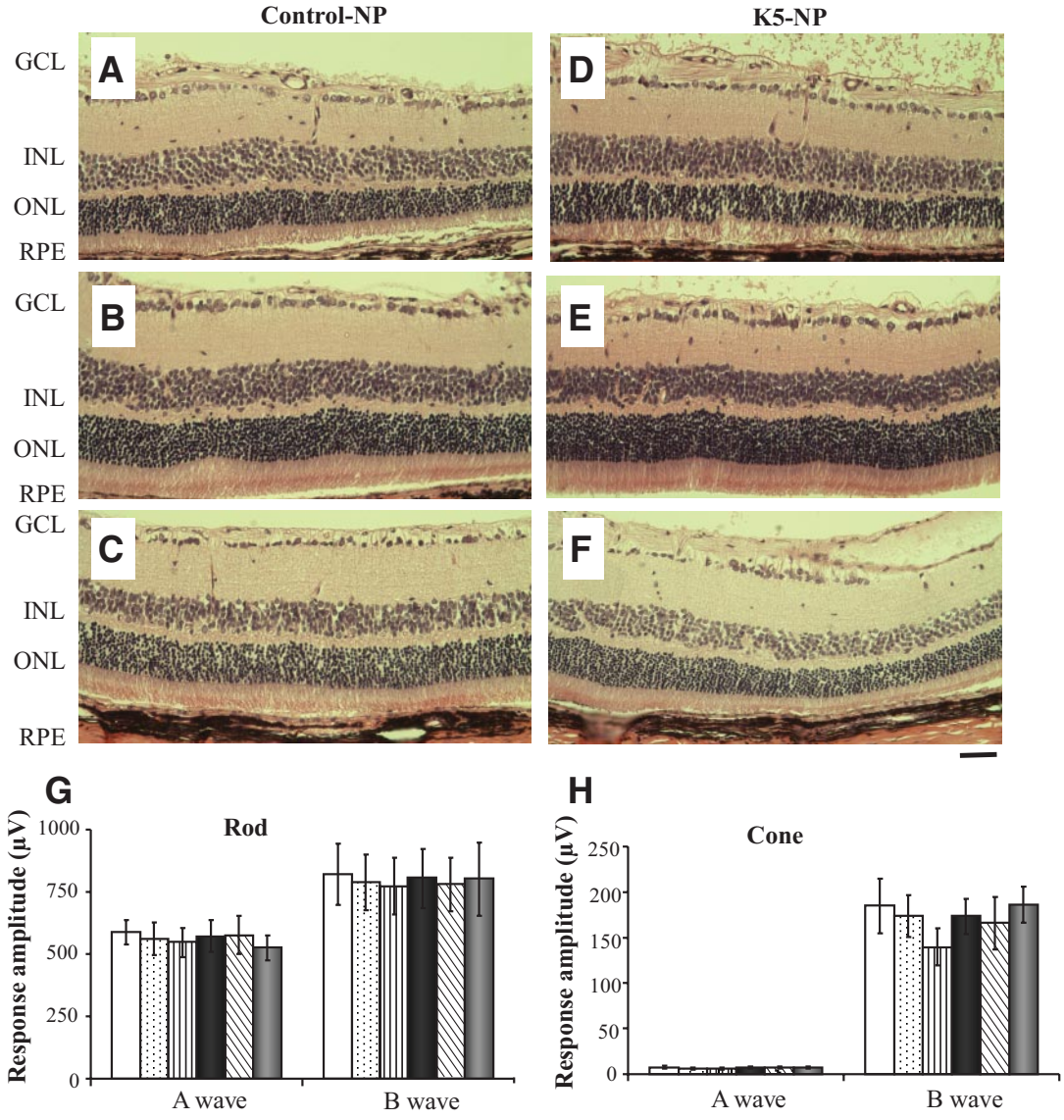

FIG. 8. Histology and ERG response in the eyes injected with K5-NP. Adult rats received an intravitreal injection of K5-NP or control-NP. The animals were killed, and the eye sections were stained with hematoxylin and eosin (three rats per time point). *A–F*: Representative images of the eyes at 1 (*A*, *D*), 2 (*B*, *E*), and 4 (*C*, *F*) weeks after the injection. Scale bar: 20 μm. *G* and *H*: ERG was recorded from six rats at 4 weeks after the injection of K5-NP and Control-NP to nondiabetic and diabetic rats and age-matched untreated nondiabetic and diabetic rats. Amplitudes of A- and B-waves from scotopic and photopic ERG were averaged and compared (mean ± SD, $n = 6$). □, Normal; ▨, normal + control-NP; ▥, normal + K5-NP; ■, STZ; ▧, STZ + control-NP; ▩, STZ + K5-NP. GCL, ganglion cell layer; INL, inner nuclear layer; ONL, outer nuclear layer; RPE, retinal pigment epithelium. (A high-quality digital representation of this figure is available in the online issue.)

increased HIF-1α levels in the nuclei (Fig. 9*A*). K5-NP, but not Control-NP, completely blocked the increase of nuclear HIF-1α levels under hypoxia (Fig. 9*A*).

Similarly, nuclear translocation of HIF-1α was also determined in the retina of the OIR rats by immunostaining of HIF-1α. OIR rats showed high levels of HIF-1α in the nuclei in the inner retina injected with Control-NP (Fig. 9*B–D*). In the contralateral eyes injected with K5-NP, the HIF-1α signal in the nuclei of retinal cells was apparently decreased (Fig. 9*E–G*), suggesting that K5-NP inhibited HIF-1α nuclear translocation.

DISCUSSION

Retinal vascular leakage, the direct cause of diabetic macular edema, and retinal neovascularization are the major causes of vision loss in diabetic patients (1). Long-term suppression of retinal vascular leakage and pathologic retinal neovascularization are the goals for the treatment of diabetic retinopathy. Although previous studies showed that peptide angiogenic factors such as K5, angiostatin, and so forth effectively reduce vascular leakage and inhibit retinal neovascularization in rat models (14,32), the difficulty in achieving sustained ocular delivery of the peptides represents a major hurdle for their therapeutic applications. The present study reports the first approach to combine an endogenous angiogenic inhibitor with nanotechnology in the treatment of diabetic retinopathy. Our results showed that an intravitreal injection of K5-NP mediated high-level and sustained K5 expression in the retina and resulted in sustained reductions of retinal vascular leakage in STZ-induced diabetic and OIR models. Further, K5-NP effectively blocked ischemia-induced retinal neovascularization. This study also identified a novel

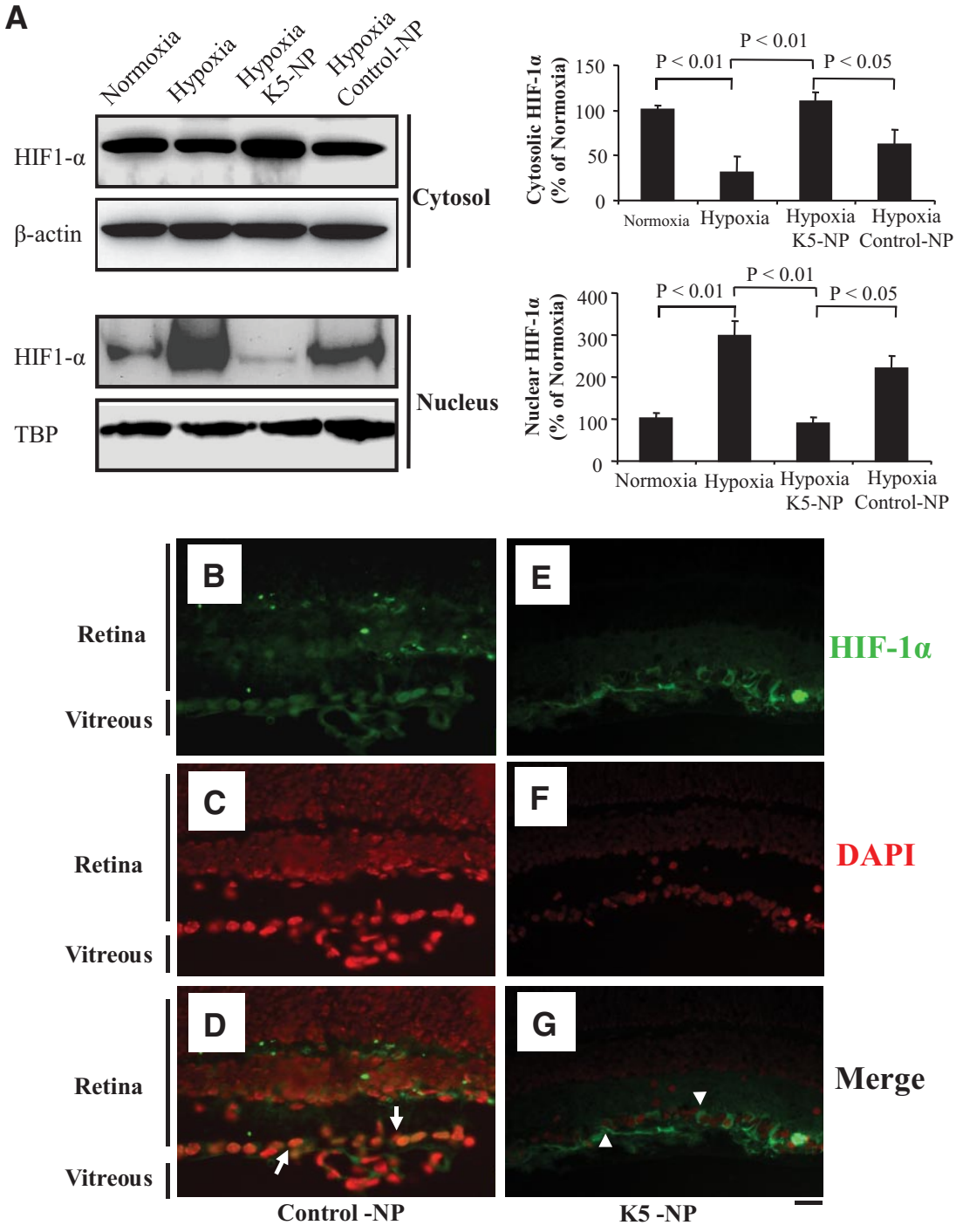

FIG. 9. Blockade of nuclear translocation of HIF-1α by K5-NP. *A*: BRCECs were treated with K5-NP or control-NP for 48 h under normoxia or hypoxia (1% oxygen). The cytosol and nucleus were isolated, and the same amount of proteins (30 μg) from each sample was used for Western blot analysis using an anti–HIF-1α antibody. The membranes were stripped and re-blotted with antibodies for β-actin and nuclear protein TBP. Cytosolic and nuclear levels of HIF-1α were semi-quantified by densitometry, normalized by β-actin and TBP, respectively, and expressed as percent of nondiabetic control (mean ± SD, $n = 3$). *B–G*: Three OIR rats received an intravitreal injection of control-NP in the left eye (*B–D*) and K5-NP into the right eye (*E–G*) at P12. The eyes were fixed and sectioned at P16. The retinal sections were stained with the antibody specific for HIF-1α (*green*) and the nuclei counterstained with DAPI (*red*). *B* and *E*: HIF-1α immunostaining; *C* and *F*: DAPI staining of the nuclei; *D* and *G*: merged images of HIF-1α and DAPI staining. Note that the nuclei with increased HIF-1α signal superimposed on DAPI staining show orange color in *D*. White arrows indicate different intensities of HIF-1α staining in the nuclei of inner retinal cells in *D* and *G*. Scale bar: 10 μm. (A high-quality digital representation of this figure is available in the online issue.)

anti-inflammatory effect of K5 in the retina of diabetic rats. Moreover, the K5-NP injection did not result in any detectable toxicity to retinal structure and function. This study revealed therapeutic potential of nanoparticle-mediated gene delivery of angiogenic inhibitors in the treatment of diabetic retinopathy.

Nanoparticles formulated using PLGA polymers are recently being investigated as a new gene delivery system because of their sustained release characteristics, biocompatibility, biodegradability, and ability to protect DNA from degradation in lysosomes (33,34). Our immunoblotting and double immunostaining results showed that

K5-NP mediated high-level and sustained K5 expression in cultured cells and in the inner retina, suggesting that K5-NP is efficiently internalized and released into the cytoplasmic compartment rather than being retained in the degradative lysosomal compartment. Moreover, the expressed K5 is secreted into the extracellular space and has biological activity of specifically inhibiting endothelial cell growth and VEGF overexpression under hypoxia and in the retina of STZ-induced diabetes.

Cytotoxicity is a potential concern in some nanoparticle-mediated gene deliveries. We have determined potential cytotoxicities of K5-NP in cultured ARP19 cells and in the retina. In ARPE19 cells treated with K5-NP, no significant reduction in cell viability was observed. In contrast, the same concentrations of K5-NP significantly inhibited endothelial cell growth, suggesting an endothelial cell-specific inhibitory effect of K5-NP. After an intravitreal injection of K5-NP, no significant alterations were observed in the retinal histology at any of the time points analyzed. Moreover, analyses of the ERG response, retinal thickness, and cell death in the retina suggest that K5-NP does not have any detectable side effects on retinal structure and functions. These data suggest that K5-NP has no severe toxicities at the dose used.

Our previous studies demonstrated that the anti-angiogenic activity of K5 is through downregulating the expression of VEGF (30). As VEGF is a major permeability and angiogenic factor, downregulation of VEGF expression is believed to be responsible for the effects of K5 on vascular leakage and retinal neovascularization (14,15). To confirm whether the expressed K5 from nanoparticles plays a role in blocking the VEGF overexpression under hypoxia, we measured VEGF expression in retinal pigment epithelium cells and Müller cells. Exposure of the cells to hypoxia increased the VEGF expression. The overexpression of VEGF under hypoxia can be effectively blocked by K5-NP, suggesting that the mechanism underlying the vascular activities of K5-NP is identical to that of the K5 peptide.

The OIR model is commonly used for studies of proliferative diabetic retinopathy (35–37). Although it is not a diabetic model, the pathology in the retina in this model is similar to that in diabetic retinopathy in humans (27). Moreover, VEGF overexpression has been shown to be the key pathogenic factor for retinal vascular leakage and neovascularization in this model, a pathogenic mechanism similar to that in diabetic retinopathy (8,38). Our results showed that K5-NP reduced retinal vascular permeability in a dose-dependent manner, demonstrating a beneficial effect on vascular leakage induced by hypoxia.

To evaluate the effect of K5-NP on retinal neovascularization in the OIR model, we used fluorescein angiography on flat-mounted retinas. The results showed that a single injection of K5-NP significantly reduced retinal neovascular area and nonperfusion area that have been shown to correlate with the severity of diabetic retinopathy (27,35). Because preretinal neovascularization (i.e., neovasculature growing into the vitreous space) is a characteristic of proliferate diabetic retinopathy, we have also evaluated the effect of K5-NP on preretinal neovascular events. The results showed that K5-NP significantly reduced preretinal neovascular cells, compared with the contralateral eyes injected with Control-NP. These results demonstrate that K5-NP attenuates ischemia-induced retinal neovascularization. A limitation of the OIR model, however, is that both the vascular leakage and retinal neovascularization are transient, with peaks at P16 and P18, respectively (27,28).

Sustained expression is a goal of gene delivery. In the entire experimental period (4 weeks), K5-NP mediated efficient expression of K5 in the retina. To evaluate the sustained effects of K5, we have used the STZ-diabetic rat model, a commonly used type 1 diabetic model. As STZ-induced diabetic rats are known to develop vascular leakage and retinal inflammation but not neovascularization, we measured the effect of K5-NP on retinal vascular leakage and inflammation in the STZ-induced diabetic model. Our results showed that K5-NP reduced retinal vascular leakage for at least 4 weeks after a single injection in diabetic rats. Further, K5-NP attenuated the overexpression of VEGF and ICAM-1, two major inflammatory factors (3,39). Further, K5-NP also decreased leukostasis in the retina of the diabetic rats. These results indicate that K5-NP has a novel anti-inflammatory activity.

In conclusion, the present study demonstrates that PLGA nanoparticles can be used for gene delivery of angiogenic inhibitors into the retina without toxicity. The nanoparticle-mediated nonviral gene delivery of angiogenic inhibitors has therapeutic potential for the treatment of diabetic macular edema and retinal neovascularization associated with several ocular disorders such as diabetic retinopathy.

ACKNOWLEDGMENTS

This study was supported by National Institutes of Health Grants EY015650, EY12231, and EY019309 to J.M. and EY017045 to U.B.K. (via Emory University); grant P20RR024215 from the National Center for Research Resources; and a grant from the Oklahoma Center for the Advancement of Science and Technology as well as research awards from the American Diabetes Association and the Juvenile Diabetes Research Foundation.

REFERENCES

1. Aiello LP, Gardner TW, King GL, Blankenship G, Cavallerano JD, Ferris FL 3rd, Klein R. Diabetic retinopathy. Diabetes Care 1998;21:143–156
2. Gardner TW, Antonetti DA, Barber AJ, LaNoue KF, Levison SW. Diabetic retinopathy: more than meets the eye. Surv Ophthalmol 2002;2(Suppl.): S253–S262
3. Kern TS. Contributions of inflammatory processes to the development of the early stages of diabetic retinopathy. Exp Diabetes Res 2007;2007:95103
4. Miller JW. Vascular endothelial growth factor and ocular neovascularization. Am J Pathol 1997;151:13–23
5. Smith LE. Pathogenesis of retinopathy of prematurity. Semin Neonatol 2003;8:469–473
6. Aiello LP, Bursell SE, Clermont A, Duh E, Ishii H, Takagi C, Mori F, Ciulla TA, Ways K, Jirousek M, Smith LE, King GL. Vascular endothelial growth factor-induced retinal permeability is mediated by protein kinase C in vivo and suppressed by an orally effective beta-isoform-selective inhibitor. Diabetes 1997;46:1473–1480
7. Aiello LP, Wong JS. Role of vascular endothelial growth factor in diabetic vascular complications. Kidney Int Suppl 2000;77:S113–S119
8. Pierce EA, Avery RL, Foley ED, Aiello LP, Smith LE. Vascular endothelial growth factor/vascular permeability factor expression in a mouse model of retinal neovascularization. Proc Natl Acad Sci U S A 1995;92:905–909
9. Gao G, Li Y, Zhang D, Gee S, Crosson C, Ma J. Unbalanced expression of VEGF and PEDF in ischemia-induced retinal neovascularization. FEBS Lett 2001;489:270–276
10. Bouck N. PEDF: anti-angiogenic guardian of ocular function. Trends Mol Med 2002;8:330–334
11. O'Reilly MS, Holmgren L, Shing Y, Chen C, Rosenthal RA, Moses M, Lane WS, Cao Y, Sage EH, Folkman J. Angiostatin: a novel angiogenesis inhibitor that mediates the suppression of metastases by a Lewis lung carcinoma. Cell 1994;79:315–328
12. Cao Y, Chen A, An SS, Ji RW, Davidson D, Llinas M. Kringle 5 of plasminogen is a novel inhibitor of endothelial cell growth. J Biol Chem 1997;272:22924–22928
13. Zhang D, Kaufman PL, Gao G, Saunders RA, Ma JX. Intravitreal injection of

plasminogen kringle 5, an endogenous angiogenic inhibitor, arrests retinal neovascularization in rats. Diabetologia 2001;44:757–765
14. Zhang SX, Sima J, Shao C, Fant J, Chen Y, Rohrer B, Gao G, Ma JX. Plasminogen kringle 5 reduces vascular leakage in the retina in rat models of oxygen-induced retinopathy and diabetes. Diabetologia 2004;47:124–131
15. Zhang SX, Sima J, Wang JJ, Shao C, Fant J, Ma JX. Systemic and periocular deliveries of plasminogen kringle 5 reduce vascular leakage in rat models of oxygen-induced retinopathy and diabetes. Curr Eye Res 2005;30:681–689
16. Kootstra NA, Verma IM. Gene therapy with viral vectors. Annu Rev Pharmacol Toxicol 2003;43:413–439
17. Acland GM, Aguirre GD, Ray J, Zhang Q, Aleman TS, Cideciyan AV, Pearce-Kelling SE, Anand V, Zeng Y, Maguire AM, Jacobson SG, Hauswirth WW, Bennett J. Gene therapy restores vision in a canine model of childhood blindness. Nat Genet 2001;28:92–95
18. Monahan PE, Jooss K, Sands MS. Safety of adeno-associated virus gene therapy vectors: a current evaluation. Expert Opin Drug Saf 2002;1:79–91
19. Tenenbaum L, Lehtonen E, Monahan PE. Evaluation of risks related to the use of adeno-associated virus-based vectors. Curr Gene Ther 2003;3:545–565
20. Vijayanathan V, Thomas T, Thomas TJ. DNA nanoparticles and development of DNA delivery vehicles for gene therapy. Biochemistry 2002;41:14085–14094
21. Farokhzad OC, Cheng J, Teply BA, Sherifi I, Jon S, Kantoff PW, Richie JP, Langer R. Targeted nanoparticle-aptamer bioconjugates for cancer chemotherapy in vivo. Proc Natl Acad Sci U S A 2006;103:6315–6320
22. Keegan ME, Saltzman WM. Surface-modified biodegradable microspheres for DNA vaccine delivery. Methods Mol Med 2006;127:107–113
23. Luo D, Saltzman WM. Synthetic DNA delivery systems. Nat Biotechnol 2000;18:33–37
24. Kumar MN, Mohapatra SS, Kong X, Jena PK, Bakowsky U, Lehr CM. Cationic poly(lactide-co-glycolide) nanoparticles as efficient in vivo gene transfection agents. J Nanosci Nanotechnol 2004;4:990–994
25. Limb GA, Salt TE, Munro PM, Moss SE, Khaw PT. In vitro characterization of a spontaneously immortalized human Muller cell line (MIO-M1). Invest Ophthalmol Vis Sci 2002;43:864–869
26. Wang JJ, Zhang SX, Lu K, Chen Y, Mott R, Sato S, Ma JX. Decreased expression of pigment epithelium-derived factor is involved in the pathogenesis of diabetic nephropathy. Diabetes 2005;54:243–250
27. Smith LE, Wesolowski E, McLellan A, Kostyk SK, D'Amato R, Sullivan R, D'Amore PA. Oxygen-induced retinopathy in the mouse. Invest Ophthalmol Vis Sci 1994;35:101–111
28. Zhang SX, Ma JX, Sima J, Chen Y, Hu MS, Ottlecz A, Lambrou GN. Genetic difference in susceptibility to the blood-retina barrier breakdown in diabetes and oxygen-induced retinopathy. Am J Pathol 2005;166:313–321
29. Xu Q, Qaum T, Adamis AP. Sensitive blood-retinal barrier breakdown quantitation using Evans blue. Invest Ophthalmol Vis Sci 2001;42:789–794
30. Gao G, Li Y, Gee S, Dudley A, Fant J, Crosson C, Ma JX. Down-regulation of vascular endothelial growth factor and up-regulation of pigment epithelium-derived factor: a possible mechanism for the anti-angiogenic activity of plasminogen kringle 5. J Biol Chem 2002;277:9492–9497
31. Zhang SX, Wang JJ, Gao G, Shao C, Mott R, Ma JX. Pigment epithelium-derived factor (PEDF) is an endogenous anti-inflammatory factor. FASEB J 2006;20:323–325
32. Sima J, Zhang SX, Shao C, Fant J, Ma JX. The effect of angiostatin on vascular leakage and VEGF expression in rat retina. FEBS Lett 2004;564:19–23
33. Cohen H, Levy RJ, Gao J, Fishbein I, Kousaev V, Sosnowski S, Slomkowski S, Golomb G. Sustained delivery and expression of DNA encapsulated in polymeric nanoparticles. Gene Ther 2000;7:1896–1905
34. Panyam J, Zhou WZ, Prabha S, Sahoo SK, Labhasetwar V. Rapid endolysosomal escape of poly (D, L-lactide-co-glycolide) nanoparticles: implications for drug and gene delivery. FASEB J 2002;16:1217–1226
35. Penn JS, Tolman BL, Henry MM. Oxygen-induced retinopathy in the rat: relationship of retinal nonperfusion to subsequent neovascularization. Invest Ophthalmol Vis Sci 1994;35:3429–3435
36. Smith LE, Shen W, Perruzzi C, Soker S, Kinose F, Xu X, Robinson G, Driver S, Bischoff J, Zhang B, Schaeffer JM, Senger DR. Regulation of vascular endothelial growth factor-dependent retinal neovascularization by insulin-like growth factor-1 receptor. Nat Med 1999;5:1390–1395
37. Spranger J, Osterhoff M, Reimann M, Mohlig M, Ristow M, Francis MK, Cristofalo V, Hammes HP, Smith G, Boulton M, Pfeiffer AF. Loss of the antiangiogenic pigment epithelium-derived factor in patients with angiogenic eye disease. Diabetes 2001;50:2641–2645
38. Antonetti DA, Barber AJ, Hollinger LA, Wolpert EB, Gardner TW. Vascular endothelial growth factor induces rapid phosphorylation of tight junction proteins occludin and zonula occluden 1: a potential mechanism for vascular permeability in diabetic retinopathy and tumors. J Biol Chem 1999;274:23463–23467
39. Masuzawa K, Jesmin S, Maeda S, Zaedi S, Shimojo N, Miyauchi T, Goto K. Effect of endothelin dual receptor antagonist on VEGF levels in streptozotocin-induced diabetic rat retina. Exp Biol Med (Maywood) 2006;231:1090–1094
40. Komeima K, Rogers BS, Campochiaro PA. Antioxidants slow photoreceptor cell death in mouse models of retinitis pigmentosa. J Cell Physiol 2007;213:809–815
41. Joussen AM, Poulaki V, Le ML, Koizumi K, Esser C, Janicki H, Schraermeyer U, Kociok N, Fauser S, Kirchhof B, Kern TS, Adamis AP. A central role for inflammation in the pathogenesis of diabetic retinopathy. FASEB J 2004;18:1450–1452
42. Zhang X, Bao S, Lai D, Rapkins RW, Gillies MC. Intravitreal triamcinolone acetonide inhibits breakdown of the blood-retinal barrier through differential regulation of VEGF-A and its receptors in early diabetic rat retinas. Diabetes 2008;57:1026–1033